DESIGN METHODS FOR DC ARC FURNACES TO ENHANCE FURNACE INTEGRITY

*R.T. Jones and Q.G. Reynolds

Pyrometallurgy Division, Mintek
200 Malibongwe Drive
Private Bag X3015, Randburg, 2125, South Africa
*(*Corresponding author: rtjones@global.co.za)*

ABSTRACT

The choice of furnace design parameters has a marked effect on the integrity of the furnace that is constructed. The design methodology for DC arc furnaces typically begins with the chemical reactions and feed materials that define the process. The specific energy requirement of the process, and the feedrates of the raw materials largely determine the power requirement for the furnace. A chosen value for the 'power intensity' sets the diameter of the furnace. Justification is provided for why this is a good choice of scale-up parameter. Equations are presented to quantify the resulting trade-off between thermal efficiency and the degree of error that can be tolerated in the balance between power and feedrate. This improved understanding should provide a better rationale for selecting an appropriate power intensity (or furnace diameter) for future furnaces.

KEYWORDS

Pyrometallurgy, DC arc furnace, power intensity, furnace integrity.

INTRODUCTION

The choices made during the design of an electrical furnace have a significant bearing on the performance and longevity of the vessel. The design specifications for DC arc furnaces (and for some other furnaces) include geometric factors (such as diameter, height, roof angle, tap-hole heights, electrode diameter), electrical factors (such as power, voltage, and current ranges), feed system (feedrate, and distribution arrangement), and refractories. DC arc furnaces have been used for a wide variety of applications (Jones, 2014), and each type of process has its own set of areas that require particular attention. Historically, some of the design parameters have been specified based on past experience and rules of thumb, and sometimes they have been based on misconceptions (Jones *et al.*, 2011).

The design process usually starts with an understanding of the chemical processes and the associated thermodynamics. The specific energy requirement (SER, usually expressed in kWh/kg) of the process is defined as the difference between the enthalpy of the products and the enthalpy of the feed materials at their respective temperatures, relative to the elements at 25°C. This, together with the required feedrate, sets the overall power requirement of the process. The overall power required for the furnace is the sum of the power requirement for the process and the power lost from the vessel (through the sidewalls and roof, for example).

The furnace diameter is usually chosen to match a pre-selected power intensity (usually measured in kW/m^2) for the given process. This intensity is often spoken of as "power density" – a terminology that usually suggests power per unit volume, even though this is not what is meant by the term. Sometimes the term "power flux" is used in place of this – but it sounds a little pretentious, even though it is technically more correct. However, we will in this paper use the term "power intensity" to refer to the total electrical power supplied to the furnace divided by the area of the upper surface of the molten slag bath. Unfortunately, it is not always explicitly clear what factors are taken into account in the choice of power intensity for a given process or furnace.

The furnace diameter is a key parameter in the furnace design, so it worth exploring whether the power intensity is a good choice of scale-up parameter.

AN ARGUMENT FOR USING POWER INTENSITY AS A SCALE-UP PARAMETER

Consider the DC arc furnace shown schematically in Figure 1. The furnace has a circular cross-section, and has a molten slag bath with an open upper surface.
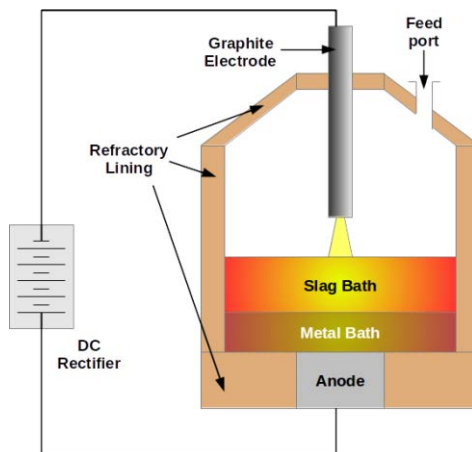

Figure 1 – Schematic of a direct-current plasma arc furnace

If it is assumed that the furnace is continuously fed through openings in the roof, and that the feed ports are relatively evenly spaced, then the open bath is subject to a constant flux of feed material falling into it. Such even spacing of the feed to a DC furnace across the entire cross-section of the vessel is not necessarily typical, but an argument similar to this may be made using a 'feed zone' or 'open-bath' diameter that is scaled relative to the full inner diameter of the furnace vessel.

Two possible feed consumption regimes may be considered.

Regime 1: Particles Sink into the Slag

In the first regime, the particles are denser than the slag, and settle below the surface faster than they are consumed. Because of the viscous nature of the molten slag, particles of feed falling into it are soon slowed to their terminal velocity. Assuming approximately spherical particles and Stokes flow, this velocity is given by Equation (1).

$$u_t = \frac{g(\rho_f - \rho_s)d_f^2}{18\mu_s} \qquad (1)$$

Here, u_t is the terminal velocity of a feed particle settling in slag under gravitational acceleration g; ρ_f and ρ_s are the feed and slag densities respectively; d_f is the particle diameter; and μ_s is the viscosity of the molten slag.

In this case, the rate of settling determines an upper limit on the total feedrate to the furnace, assuming that an open-bath operation is to be maintained.

$$\dot{m}_{f,max} = \rho_f(1-\varepsilon)u_t A_c \qquad (2)$$

Here, $\dot{m}_{f,max}$ is the maximum feedrate above which feed will accumulate on the surface of the bath, resulting in covered operation, ε is the void fraction of a bed of feed particles, and A_c is the cross-sectional area of the furnace vessel (upper surface area of the slag bath).

Regime 2: Particles are Consumed at the Surface

In the second regime, feed particles are consumed at the slag surface before they have a chance to sink into the bath. Here, the feed particles have an associated 'survival time', τ_f, after which they either melt or dissolve into, or are chemically consumed by, the slag. In this case, the maximum number of particles that the bath is able to consume in τ_f seconds is given by n_p.

$$n_p = \frac{(1-\varepsilon_{2D})A_c}{\frac{\pi}{4}d_f^2} \qquad (3)$$

Here, ε_{2D} is the void fraction of a two-dimensional layer of feed particles covering the slag bath surface, typically ~0.9. The maximum feedrate may then be determined as shown in Equation (4).

$$\dot{m}_{f,max} = \frac{\frac{\pi}{6}d_f^3\rho_f n_p}{\tau_f} = \frac{2}{3}\rho_f(1-\varepsilon_{2D})\frac{d_f}{\tau_f}A_c \qquad (4)$$

It is interesting to note that, in both regimes, shown in Equations (2) and (4), the maximum feedrate possible before the operation ceases to be open-bath is proportional to the surface area of the slag bath A_c. It would, therefore, seem reasonable to scale up an operation that works suitably at pilot scale by using 'feedrate per unit cross-sectional area', $\dot{m}_f / A_c$, as an invariant.

The total power input, P_f, to a DC furnace may be separated into a feed-consumption component and a losses component, Q_L, as shown in Equation (5).

$$P_f = \dot{m}_f \; SER + Q_L \qquad (5)$$

As the thermal efficiency of DC arc furnaces at both pilot- and industrial-scale is generally high ($> 80\%$), furnace power P_f may be approximated as roughly proportional to feedrate $\dot{m}_f$, for the purposes of scale-up calculations. Furthermore, if we make the reasonable assumption here that the process chemistry (and therefore the specific energy requirement) remains the same across process scales, the invariant 'feedrate per unit cross-sectional area', $\dot{m}_f / A_c$, can be multiplied by the SER and still remain invariant. In this case, the power intensity, P_f / A_c, may be seen to be also approximately invariant.

$$\frac{\dot{m}_f}{A_c} SER \approx \frac{P_f}{A_c} \qquad (6)$$

Scaling DC furnaces using a constant power intensity is therefore a reasonable approximation, and would serve to maintain similar feed-assimilation conditions in furnaces of different sizes; scaling according to 'feedrate per unit cross-sectional area' would, however, be a somewhat more rigorous approach.

SEMI-EMPIRICAL MODELLING OF THE SLAG BATH

A simple energy balance may be constructed around the furnace slag bath and is of some value in exploring the implications of changing certain design variables. This energy balance is shown schematically in Figure 2.
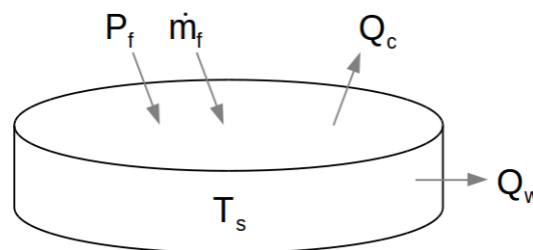

Figure 2 – Inputs and outputs for slag-bath energy balance

The slag bath receives energy input from the plasma arc at the furnace power setting P_f, and also receives feed at a rate of $\dot{m}_f$. The open upper surface of the slag bath loses energy by radiation to the upper sidewalls and roof at a rate Q_c, and by convection to the freeze lining and lower sidewall refractories at a rate of Q_w. For the purposes of the present model, it is assumed that the lower surface of the slag bath is insulating, although this is generally not entirely true as some losses will occur via the furnace hearth. The energy balance then sets the slag temperature T_s and the freeze lining thickness x_{fl}.

If the assumption is made that radiative energy transfer between the slag-bath surface and the inner surface of the freeboard refractories is "very good" (Reynolds, 2002), then the 'heat transfer resistance' of the refractories dominates the overall 'heat transfer resistance' between bath surface and cooling system in the freeboard. Q_c may therefore be approximated by Equation (7).

$$Q_c \approx \frac{k_{fb}}{x_{fb}} \frac{A_{fb}}{A_c} A_c (T_s - T_\infty) = U_{fb} A_c (T_s - T_\infty) \tag{7}$$

Here, k_{fb} and x_{fb} are the thermal conductivity and thickness of the freeboard refractory layer respectively; A_{fb} is the inner surface area of the freeboard refractory lining; and T_∞ is the temperature of the cooling medium outside the refractory layer. U_{fb} is the compound heat transfer resistance between the slag-bath surface and the cooling medium, in this case approximated as the resistance of the freeboard refractory layer.

For energy losses through the furnace sidewalls, the presence of a freeze lining of solid slag with variable thickness results in two heat transfer resistances in series. Q_w is therefore given by both of the following expressions (8a) and (8b).

$$Q_w = h_w A_w (T_s - T_{MPT}) \tag{8a}$$

$$Q_w = \frac{1}{\dfrac{x_{fl}}{k_{fl}} + \dfrac{x_w}{k_w}} A_w (T_{MPT} - T_\infty) \tag{8b}$$

Here, h_w is the convective heat transfer coefficient between the bulk molten slag and the surface of the freeze lining; A_w is the surface area of the sidewall in contact with the slag bath; T_{MPT} is the effective melting temperature of the slag (somewhere between the liquidus and solidus temperatures); x_w and k_w are the thickness and thermal conductivity of the sidewall refractory; and x_{fl} and k_{fl} are the thickness and thermal conductivity of the freeze lining. The heat transfer resistance between the outer surface of the refractory and the cooling medium is assumed to be negligible, and the thicknesses of both the refractory layer and the freeze lining are assumed to be small in comparison to the diameter of the furnace.

Using Equations (5), (7), and (8), two further equations may be formed from the energy balance around the slag layer.

$$P_f - \dot{m}_f SER = U_{fb} A_c (T_s - T_\infty) + h_w A_w (T_s - T_{MPT}) \tag{9a}$$

$$h_w A_w (T_s - T_{MPT}) = \frac{1}{\dfrac{x_{fl}}{k_{fl}} + \dfrac{x_w}{k_w}} A_w (T_{MPT} - T_\infty) \tag{9b}$$

By substituting in expressions for the areas as a function of the furnace dimensions and simplifying, the following expressions result from Equations (9a) and (9b). Here, D_f is the furnace diameter at the slag surface; and H_w is the depth of the slag bath.

$$P_f - \dot{m}_f SER = \frac{\pi}{4} D_f^2 U_{fb} (T_s - T_\infty) + \pi D_f H_w h_w (T_s - T_{MPT}) \tag{10a}$$

$$\frac{T_{MPT} - T_\infty}{T_s - T_{MPT}} = h_w \left(\frac{x_{fl}}{k_{fl}} + \frac{x_w}{k_w} \right)$$ (10b)

The first equation, (10a), relates the slag temperature to the power input and feedrate of the furnace, and the second, (10b), relates the slag temperature to the freeze lining thickness.

Two significant points should be noted. Firstly, although it is very simple, this model distinguishes between parameters that are largely scale-independent, such as heat transfer coefficients and operating temperatures, and those that are not, such as furnace power, feedrate, and dimensions. Secondly, the energy balance allows for any amount of power to be put into a furnace vessel of any size, provided the power input is correctly balanced with the incoming feed, such that the desired freeze lining thickness is obtained. It is perfectly plausible, for example, to run a furnace of 1 m diameter at 50 MW and maintain both a suitable freeze lining on the sidewalls and the desired slag temperature; however, the furnace's *sensitivity to operational error* will be extremely large, and small mistakes or imbalances will have potentially catastrophic consequences.

EFFECT OF DESIGN PARAMETERS ON SENSITIVITY OF OPERATION AND EFFICIENCY

In order to study the effect of a furnace's design parameters on its sensitivity to operation, it is of some interest to further explore variables derived from the model. The rate of change of the furnace freeze lining with power input, which is calculated by combining Equations (10a) and (10b) into a single expression and taking the appropriate partial derivative, may be calculated as follows.

$$\frac{\partial x_{fl}}{\partial P_f} = - \frac{k_{fl} \left(\dfrac{D_f U_{fb}}{4} + H_w h_w \right)(T_{MPT} - T_\infty)}{\pi D_f h_w \left[\dfrac{P_f - \dot{m}_f SER}{\pi D_f} - \dfrac{D_f U_{fb}}{4}(T_{MPT} - T_\infty) \right]^2}$$ (11)

This value gives an indication of how much the freeze lining melts back or grows with variations in the power input, assuming a fixed feedrate and other parameters. In particular, the dependence of the freeze lining rate of change on furnace diameter, D_f, is a rather complicated rational function, but inspection of Equation (11) shows that it decreases monotonically with increasing D_f. Smaller furnaces with higher power intensities will therefore be more sensitive to power fluctuations, and *vice versa*.

Related to this sensitivity are the 'allowable errors' in power and feedrate. These are calculated from the critical power or feedrate at which the freeze lining disappears entirely, and molten slag comes into direct contact with the sidewall refractories. This is assumed to be an undesirable and dangerous condition. Using Equations (10a) and (10b) with x_{fl} set to zero gives Equations (12a) and (12b).

$$P_{f,crit} = \dot{m}_f SER + \left[\frac{\pi}{4} D_f^2 U_{fb} \left(1 + \frac{k_w}{h_w x_w} \right) + \pi D_f H_w \frac{k_w}{x_w} \right](T_{MPT} - T_\infty)$$ (12a)

$$\dot{m}_{f,crit} = \frac{1}{SER} \left(P_f - \left[\frac{\pi}{4} D_f^2 U_{fb} \left(1 + \frac{k_w}{h_w x_w} \right) + \pi D_f H_w \frac{k_w}{x_w} \right](T_{MPT} - T_\infty) \right)$$ (12b)

The allowable errors are then defined as follows:

$$\delta P_f = \left| 1 - \frac{P_{f,crit}}{P_f} \right| \tag{13a}$$

$$\delta \dot{m}_f = \left| 1 - \frac{\dot{m}_{f,crit}}{\dot{m}_f} \right| \tag{13b}$$

It can be seen that the allowable errors in power and feedrate increase monotonically with increasing furnace diameter D_f. This again indicates that, at a given power rating, larger furnaces with lower power intensities will have more leeway for operator and control error than do smaller furnaces.

It is also of some interest to examine the dependence of the furnace's thermal efficiency, η_f, on various parameters. This is calculated simply as the fraction of the furnace power that is used by the process.

$$\eta_f = 1 - \frac{Q_c + Q_w}{P_f} = \frac{\dot{m}_f\,SER}{P_f} \tag{14}$$

From Equation (10a), it can be seen that, for a fixed target slag temperature, the difference between $\dot{m}_f\,SER$ and P_f becomes monotonically smaller with decreasing furnace diameter. This indicates that smaller furnaces, while being more sensitive to error, will run at higher efficiencies for a given required power or feedrate. The preferred power intensity and furnace diameter for any given pyrometallurgical process will therefore involve a trade-off between operability and efficiency.

EXAMPLE RESULTS AND DISCUSSION

To illustrate the functioning of the semi-empirical model more clearly, example calculations are presented for a DC furnace process at both pilot and industrial scale. The parameters used for both are shown in Table 1.

Table 1 – Fixed parameters used in furnace model calculations

Fixed Parameter	Value - pilot	Value - industrial
Feedrate, $\dot{m}_f$	3 t/h	35 t/h
Slag temperature, T_s	1550°C	1550°C
Specific energy requirement, SER	0.7 MWh/t	0.7 MWh/t
Sidewall refractory thermal conductivity, k_w	5 W/mK	5 W/mK
Freeboard refractory thermal conductivity, k_{fb}	1.5 W/mK	1.5 W/mK
Freeze lining thermal conductivity, k_{fl}	2.5 W/mK	2.5 W/mK
Sidewall refractory thickness (minimum), x_w	0.11 m	0.11 m
Freeboard refractory thickness, x_{fb}	0.15 m	0.25 m
Freeboard:bath area ratio, A_{fb}/A_c	2	2
Slag heat transfer coefficient, h_w	200 W/m²K	200 W/m²K
Slag melting point, T_{MPT}	1450°C	1450°C
Coolant temperature, T_∞	25°C	25°C
Slag bath depth, H_w	0.4 m	0.75 m

With these parameters, the freeze lining thickness is calculated as 0.123 m at both scales, assuming that the sidewall refractory has worn back to its minimum thickness. The effective freeboard heat transfer coefficient U_{fb} is calculated as 20 W/m²K at pilot scale, and 12 W/m²K at industrial scale.

The effect of changing the power intensity, while keeping all other variables in Table 1 constant, was studied by varying the furnace diameter, D_f, and calculating the resulting energy losses, furnace power, and other parameters required to sustain the operation.

The results for the pilot-scale furnace model are shown in Figures 3 to 6.
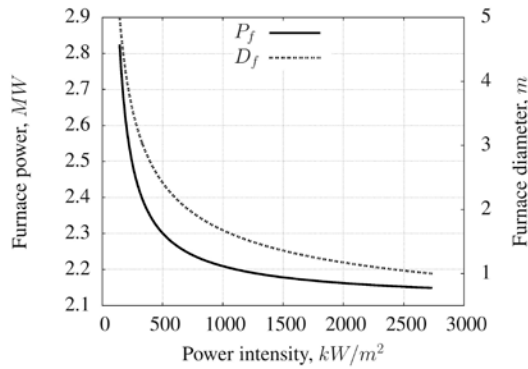
Figure 3 – Variation of required power, and furnace diameter, with power intensity
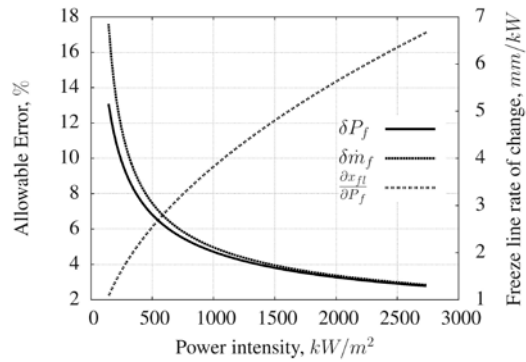
Figure 4 – Variation of allowable errors (in power and feedrate), and freeze lining rate of change, with power intensity
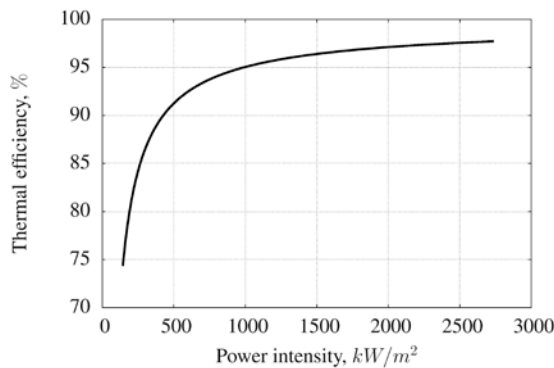

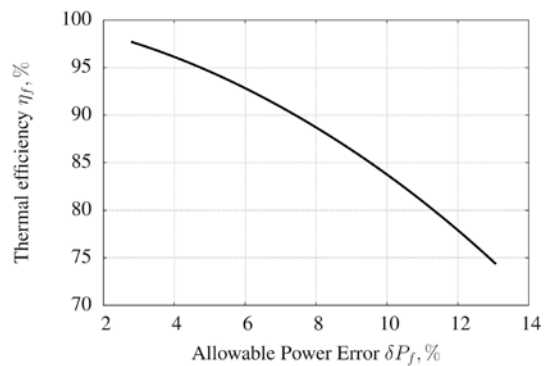Figure 5 – Variation of furnace thermal efficiency with power intensity

Figure 6 – Relationship between thermal efficiency and allowable percentage error in power

For the industrial-scale case, the results are shown in Figures 7 to 10.
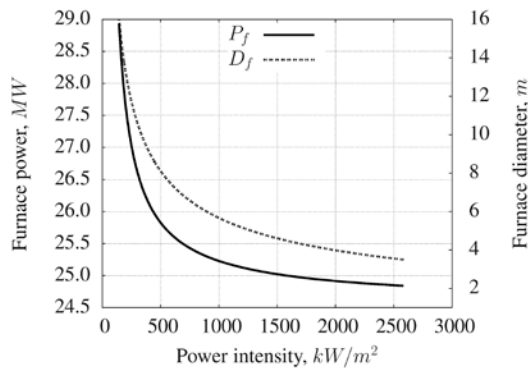

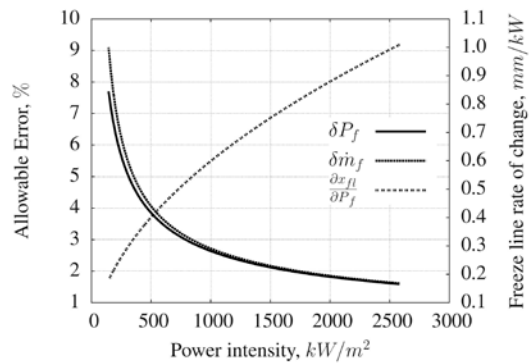Figure 7 – Variation of required power, and furnace diameter, with power intensity

Figure 8 – Variation of allowable errors (in power and feedrate), and freeze lining rate of change, with power intensity
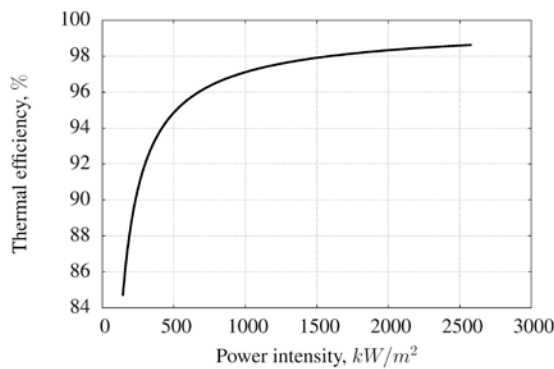

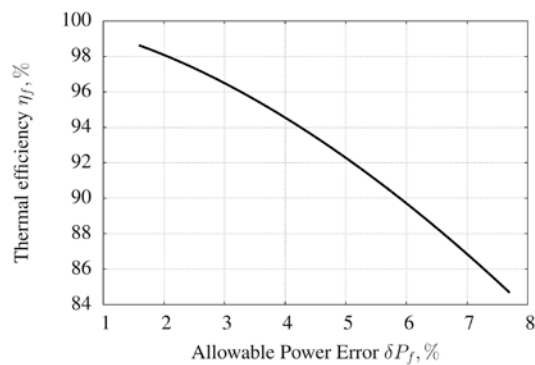Figure 9 – Variation of furnace thermal efficiency with power intensity

Figure 10 – Relationship between thermal efficiency and allowable percentage error in power

Some interesting trends may be observed in the results from the furnace models. At larger furnace diameters (smaller power intensities) at both scales, the power needed to maintain the required smelting temperature for a fixed feedrate increases sharply, and as a result the efficiency of the furnace drops off. At the same time, the various measures of sensitivity of the furnace also decrease with increasing furnace diameter (decreasing power intensity), bearing out the earlier statement that, for a given process, a smaller, more intense furnace will operate at higher efficiencies but will also be more sensitive to operator and control error.

For process optimization purposes, it is of some value to consider the relationship between the furnace's thermal efficiency and its sensitivity. This is shown for a pilot-scale furnace in Figure 6, and for an industrial-scale furnace in Figure 10, with the data parameterized by the power intensity. Using an objective function involving an appropriate combination of these two factors would then enable the optimal power intensity (and hence furnace design) for the process to be determined.

CONCLUSIONS

It is a reasonable approximation to use power intensity as a scale-up factor, although it would be slightly more rigorous to use feedrate flux instead.

Although it is theoretically possible to operate a furnace at any given power intensity (as long as the power and feedrate are perfectly balanced), in practice the furnace's sensitivity to operational error will vary widely with power intensity. There is an engineering trade-off between the thermal efficiency of the furnace and the degree of error that can be tolerated in the balance between power and feedrate. The equations presented here make it possible to quantify these effects. This improved understanding should provide a better rationale for selecting an appropriate power intensity (or furnace diameter) for future furnaces.

ACKNOWLEDGEMENTS

REFERENCES

Jones R.T. (2014). DC arc furnaces – Past, present, and future, *Celebrating the Megascale, Proceedings of the Extraction and Processing Division Symposium on Pyrometallurgy in Honor of David G.C. Robertson*, TMS 2014, 16-20 February 2014, San Diego, California, USA, pp.129-139. http://www.mintek.co.za/Pyromet/Files/2014Jones-DCArcFurnaces.pdf

Jones R.T., Reynolds Q.G., Curr T.R., and Sager D. (2011). Some myths about DC arc furnaces, *Journal of the SAIMM*, Vol. 111, Number 10, October 2011, pp.665-673. http://www.mintek.co.za/Pyromet/Files/2011Jones2.pdf

Reynolds Q.G. (2002). Thermal radiation modelling of DC smelting furnace freeboards, *Minerals Engineering*, Vol. 15, Issue 11S1, pp.993-1000. http://www.mintek.co.za/Pyromet/Files/Radiation.pdf